

**PHENOMENOLOGICAL NUCLEAR-REACTION  
DESCRIPTION IN DEUTERIUM-SATURATED  
PALLADIUM AND SYNTHESIZED STRUCTURE  
IN DENSE DEUTERIUM GAS  
UNDER  $\gamma$ -QUANTA IRRADIATION**

*A. Yu. Didyk*<sup>a, 1</sup>, *R. Wiśniewski*<sup>b, 2</sup>

<sup>a</sup> Joint Institute for Nuclear Research, Dubna

<sup>b</sup> National Center of Nuclear Research, Otwock, Poland

The observed phenomena on changes of chemical compositions in previous reports [1,2] allowed us to develop a phenomenological nuclear fusion–fission model with taking into consideration the elastic and inelastic scattering of photoprotons and photoneutrons, heating of surrounding deuterium nuclei, following  $d-d$  fusion reactions and fission of middle-mass nuclei by «hot» protons, deuterons and various-energy neutrons. Such chain processes could produce the necessary number of neutrons, «hot» deuterons for explanation of observed experimental results [1,2]. The developed approach can be a basis for creation of deuterated nuclear fission reactors (DNFR) with high-density deuterium gas and the so-called deuterated metals. Also, this approach can be used for the study of nuclear reactions in high-density deuterium or tritium gas and deuterated metals.

Обнаруженные в предыдущих работах [1,2] эффекты по изменению химического состава насыщенного дейтерием палладия и синтезированной структуры позволяют ввести феноменологические реакции слияния легких и деления более тяжелых ядер за счет упругого и неупругого рассеяния фотопротонов и фотонейтронов, с одной стороны, нагревающих окружающий плотный газ атомов и молекул дейтерия, а с другой стороны, участвующих в  $d-d$ -реакциях слияния легких и деления ядер средних масс протонами и дейтронами достаточной энергии, а также нейтронами различных энергий. Такие цепочноподобные процессы могут создать значительное число нагретых дейтронов для протекания необходимого количества ядерных реакций деления и, следовательно, позволить объяснить наблюдаемые экспериментальные результаты по накоплению легких химических элементов как продуктов ядерных реакций [1,2].

Развитый подход может быть основой для создания дейтерированных ядерных реакторов деления (ДЯРД) на основе дейтерированных металлов в плотном газообразном дейтерии. Этот подход может также быть важным с точки зрения изучения ядерных реакций в плотных тритиевом и дейтериевом газе и дейтерированных материалах.

PACS: 13.60.-r

---

<sup>1</sup>E-mail: didyk@jinr.ru

<sup>2</sup>E-mail: roland.wisniewski@gmail.com

## INTRODUCTION

The results of surface studies and x-ray elemental analysis of Pd rod and synthesized novel structure (SNO) together with changes of SNO-brass substrate, input beryllium bronze «window» and cut separating manganin sleeve at dense deuterium gas after the action of 8.8-MeV  $\gamma$  quanta were presented in our earlier papers [1, 2]. The observed chemical-composition strong changes in all components can be described by photodisintegration of deuterons under  $\gamma$  quanta, following «heating» of deuterium atoms by photoneutrons and photoprotons, development of  $d-d$  fusion and, as a result, creation of chain heating fusion–fission reactions and, as a result, strong multiplication of the hot protons numbers. These processes should be under realizing with accompanying middle-mass nuclei fission and release of energy from nuclear fission process. The efficiency of this process should be higher than unit ( $\eta \gg 1$ ).

### 1. DESCRIPTION AND CALCULATIONS OF SOME EXPERIMENTAL VALUES [1, 2]

As is known, the cross section of deuteron photodisintegration producing neutrons and protons is rather well studied, while the corresponding cross sections of  $d(\gamma, n)p$  reactions were measured experimentally and described theoretically [3, 4].

Below, an alternative approach is considered for the use of deuterium photodisintegration reactions produced in dense and superdense molecular deuterium gas under the action of  $\gamma$  quanta. In each act of deuteron fission, a neutron and proton are generated with energies defined by the reaction kinematics and energy–momentum conservation law. The energy dependence of the deuteron photodisintegration cross section from the reaction



can be quite well described by the Bethe–Peierls formula [3, 4]:

$$\sigma_{d(\gamma, n)p} = \frac{8\pi}{3} \frac{e_0^2 \hbar}{M c_0} \sqrt{\Delta W} \frac{(E_\gamma - \Delta W)^{3/2}}{E_\gamma^3}, \quad (2)$$

where  $e_0, c_0$  and  $M$  are the elementary charge, velocity of light, and nucleon mass, respectively, and  $\Delta W = 2.22$  MeV is the deuteron bond energy. In this case, reaction (1) yields a neutron and a proton with approximately equal energies, i.e.,  $E_n \approx E_p = 0.5(E_\gamma - \Delta W)$ , since the momentum of  $\gamma$  quanta is small. As is seen, the maximum cross section of the  $d(\gamma, n)p$  reaction is reached at  $E_\gamma = 2\Delta W = 4.4$  MeV and makes up  $\sigma_{d(\gamma, n)p}^{\max} = 2.4$  mb.

Energetic spectra of  $\gamma$  quanta  $N_\gamma(E_\gamma)$  were calculated from the expressions presented in [5, 6] just with own approximations of experimental values using the expression

$$N_\gamma(E_\gamma) = (c_0 + c_1 E_\gamma) \left( \frac{E_\gamma}{E_\gamma^{\max}} \right)^{\alpha_0 + \alpha_1 E_\gamma} \left( 1 - \frac{E_\gamma}{E_\gamma^{\max}} \right)^\beta. \quad (3)$$

Two sets of coefficients were obtained with the use of least square method (LSM):  $c_0 = -5.824 \cdot 10^{-3}$ ,  $c_1 = 7.1865 \cdot 10^{-2}$ ,  $\alpha_0 = -1.2690$ ,  $\alpha_1 = 0.36355$ ,  $\beta = 1.7773$ , for  $E_\gamma < 8.789$  MeV (with  $\chi^2 = 7.618$ ) and  $c_0 = -5.824 \cdot 10^{-3}$ ,  $c_1 = 0.18477$ ,  $\alpha_0 = -1.2690$ ,  $\alpha_1 = 3.2489 \cdot 10^{-2}$ ,  $\beta = 2.0282$  for  $E_\gamma < 23.0$  MeV (with  $\chi^2 = 2.226$ ).

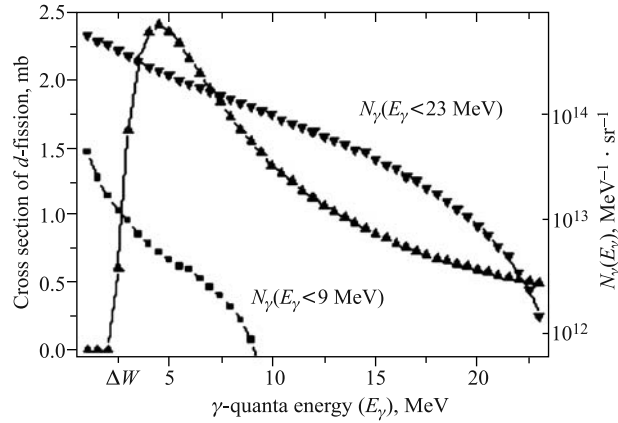


Fig. 1. Energetic dependences cross section of deuteron photodisintegration  $\sigma_{d(\gamma,n)p}$  (mb) and spectra of  $\gamma$  quanta  $N_\gamma(E_\gamma)$  ( $\text{MeV}^{-1} \cdot \text{sr}^{-1}$ ) for two maximum energies  $E_\gamma^{\text{max}} = 9.0$  MeV and  $E_\gamma^{\text{max}} = 23.0$  MeV

Figure 1 shows the cross-section of the deuteron photodisintegration  $\sigma_{d(\gamma,n)p}$  and energy spectra of  $\gamma$  quanta at the electron beam current  $J = 1 \mu\text{A}$  ( $6.25 \cdot 10^{12} \text{ s}^{-1}$ ) and  $E_\gamma < 8.8$  MeV and  $E_\gamma < 23.0$  MeV energies.

It should also be noted that during the irradiation by  $\gamma$  quanta the DHPC was cooled by a flux of compressed air at the temperature  $\approx 20^\circ\text{C}$ ; nevertheless, the temperature of the DHPC external surface significantly exceeded  $100^\circ\text{C}$  even though temperature measurements were not undertaken. Let us calculate the maximum absorbed energy of  $\gamma$  quanta per  $1 \mu\text{A}$ . The experimentally measured absorbed energy for MT-25 versus distance between the braking W target and accelerator is presented in Fig. 2. The relations between radiation energy electron loss and ionization energy loss can be described by the expression

$$\frac{S_{\text{rad}}(E_\gamma, Z)}{S_{\text{ioniz}}(E_\gamma, Z)} = \frac{E_\gamma Z}{800}; \quad (4)$$

here  $E_\gamma$  is measured in MeV. Let us estimate maximum energies absorbed by targets: the energy of our experiment  $E_\gamma^{\text{max}} = 8.8$  MeV and the other measured energy  $E_\gamma^{\text{max}} = 23.0$  MeV. To do this, it is necessary to calculate integrals using

$$E_{\text{abs. dose}}(E_\gamma^{\text{max}}) = \beta_1 \int_0^{E_\gamma^{\text{max}}} E_\gamma \frac{dN(E_\gamma)}{dE} dE_\gamma. \quad (5)$$

Parameter  $\beta$  takes into consideration an angle and distance decreasing of  $\gamma$ -quanta flux on the target, namely,  $\beta \approx 0.02$  [1, 2], but for heating of the whole DHPC it is possible to multiply this value by a factor of 10, i.e.,  $\beta_1 \approx \beta(10-20)$ . Then the absorbed power of  $\gamma$ -quanta flux

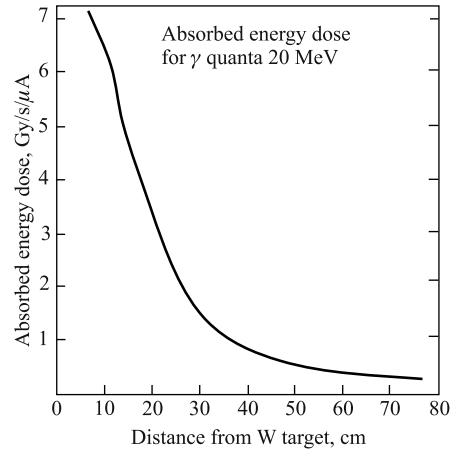


Fig. 2. Experimentally measured dose of energy versus the distance between the irradiated target and W braking target

on DHPC after integration of Eq. (5) should be

$$E_{\text{abs.dose}}(E_{\gamma}^{\text{max}} = 8.9 \text{ MeV}) = (10-20) \cdot 4.8 \cdot 10^{-2} \text{ J/(s} \cdot \mu\text{A)} \cdot 7 \mu\text{A} = (3.36-6.72) \text{ W.}$$

At electron current  $I_e = 7 \mu\text{A}$ , one can obtain  $W = (3.36-6.72) \text{ W}$ . Analogous value for the other energy can be presented

$$E_{\text{abs.dose}}(E_{\gamma}^{\text{max}} = 23 \text{ MeV}) = (10-20) \cdot 2.07 \cdot 10^{-1} \text{ J/s}/\mu\text{A}.$$

Using the expression (4), one can obtain that  $\frac{S_{\text{rad}}(E_{\gamma}, Z)}{S_{\text{ioniz}}(E_{\gamma}, Z)} = \frac{E_{\gamma}Z}{800} = \frac{8.9 \cdot 29}{800} \approx 0.32$ .

The electron beam power at  $I = 7 \mu\text{A}$  and energy  $E = 7 \text{ MeV}$  should be about  $W \approx 50 \text{ W}$ . There is a difference between power of electron beam and  $\gamma$ -quanta flux on DHPC, but these values are not very different.

The time of HPC exposure to  $\gamma$  quanta  $T \approx 2.22 \cdot 10^4 \text{ s}$  at the average current of the electron beam on the braking W target  $\bar{I}_{e-} \approx 7 \mu\text{A}$  (i.e., the average number of electrons  $\bar{N}_{e-} \approx 4.375 \cdot 10^{13} \text{ s}^{-1}$ ).

The total  $\gamma$ -quanta fluxes are presented in Table 1 for: a) total yield at  $E_{\gamma} > 0.0 \text{ MeV}$ ; b) yield with energy higher than the threshold energy of  ${}^9_4\text{Be}(\gamma, n){}_4^8\text{Be}$  reaction  $E_{\gamma} > 1.67 \text{ MeV}$ ; c) yield with energies higher than the bond energy of deuteron, i.e.,  $E_{\gamma} > \Delta W = 2.22 \text{ MeV}$ , and also yield with minimal threshold energy for W braking target  $E_{\gamma} > 6.190 \text{ MeV}$ , reaction  ${}^{183}_{74}\text{W}(\gamma, n){}^{182}_{74}\text{W}$ . The other reactions have the following energies:  ${}^{182}_{74}\text{W}(\gamma, n){}^{181}_{74}\text{W} - E_{\gamma} > 8.062 \text{ MeV}$ ,  ${}^{184}_{74}\text{W}(\gamma, n){}^{183}_{74}\text{W} - E_{\gamma} > 7.411 \text{ MeV}$  and  ${}^{186}_{74}\text{W}(\gamma, n){}^{185}_{74}\text{W} - E_{\gamma} > 7.199 \text{ MeV}$ .

The defect mass values for calculations of energetic yields and other needed parameters were taken from the handbook [7].

**Table 1. Total  $\gamma$ -quanta yield ( $\text{MeV}^{-1} \cdot \text{sr}^{-1}$ ) versus on threshold  $(\gamma, n)$  reactions for two used energetic intervals for electron current of about  $1 \mu\text{A}$**

Maximum energy of $\gamma$ quanta	$E_{\gamma} > 0.0 \text{ MeV}$	$E_{\gamma} > 1.67 \text{ MeV}$	$E_{\gamma} > 2.22 \text{ MeV}$	$E_{\gamma} > 6.19 \text{ MeV}$
$E_{\gamma}^{\text{max}} = 8.789 \text{ MeV}$	$7.45 \cdot 10^{12}$	$3.05 \cdot 10^{12}$	$2.36 \cdot 10^{12}$	$2.46 \cdot 10^{11}$
$E_{\gamma}^{\text{max}} = 23 \text{ MeV}$	$4.24 \cdot 10^{13}$	$1.85 \cdot 10^{13}$	$1.39 \cdot 10^{13}$	$2.77 \cdot 10^{12}$

Let us consider the neutron yield from some materials involved in MT-25 construction. Clearly, it should be extracted from W braking target, because the energy threshold of  $(\gamma, n)$  reactions is changed from 6.19 to 8.062 MeV (see above), and from beryllium bronze  $\text{Cu}_{0.98}\text{Be}_{0.02}$ . It is necessary to note that the yield from W target should not be significant, because the total flux of  $\gamma$  quanta is about  $N(E_{\gamma}) \equiv \frac{\partial^2 N}{\partial E \partial \Omega} \propto 2.46 \cdot 10^{11} \text{ MeV}^{-1} \cdot \text{sr}^{-1}$

at  $6.19 < E_{\gamma} < 8.789 \text{ MeV}$ . Let us estimate neutron yield of  ${}^9_4\text{Be}$  nuclei from beryllium bronze from reaction  $\gamma + {}^9_4\text{Be} \rightarrow n + {}^8_4\text{Be} \rightarrow n + {}^4_2\text{He} + {}^4_2\text{He}$  for threshold energy  $E_{\gamma} > 1.67 \text{ MeV}$ , and the cross section of the reaction is about  $\sigma_{\gamma, n} \approx 0.2 \text{ mb}$ . So the total numbers of neutrons from this reaction should take into account the total flux of  $\gamma$  quanta  $n_{\text{Be}} \approx \beta \sigma_{\gamma, n}^{\text{Be}} N_{\text{Be}} N_{\gamma}(E_{\gamma} > 1.67 \text{ MeV}) \propto 2 \cdot 10^4 \text{ s}^{-1} \cdot \mu\text{A}^{-1}$ .

We now calculate the number of neutrons and protons produced at the passage of  $\gamma$  quanta with the maximal energy  $E_\gamma < 8.789$  MeV (generated by electrons with the maximal energy  $E_e = 9.3$  MeV at the electron current beam  $J = 1 \mu\text{A}$ ) using the expression

$$Y(E_\gamma^{\max}) = \sum_{i=I_{\min}}^{i=I_{\max}} Y_i = \sum_{i=I_{\min}}^{i=I_{\max}} \beta N_D \int_{E_\gamma^i}^{E_\gamma^{i+1}} \sigma_{d(\gamma,n)p}[E_\gamma] N_\gamma[E_\gamma] dE_\gamma, \quad (6)$$

where  $E_\gamma^{I_{\min}} = \Delta W$ ,  $E_\gamma^{I_{\max}} = E_\gamma^{\max} = 9.22$  MeV, while  $E_\gamma^i = (i-1)\Delta E_\gamma + \Delta W$ , where  $i = 1, 2, \dots, 8$ ,  $I_{\max} = (9.22 - \Delta W)/\Delta E = 7$  at  $\Delta E = 1$  MeV. Figure 3 shows histograms with the number of neutrons and protons in 7 (at  $E_\gamma^{\max} = 9.3$  MeV) and 21 energy ranges ( $E_\gamma^{\max} = 23$  MeV) from reaction (1), using (2) and (3), at the electron current on the braking target  $J = 1 \mu\text{A}$ . Neutron and proton yields  $N_n(E_\gamma)$  and  $N_p(E_\gamma)$ , respectively, are also presented for two energies of electron beams of 1  $\mu\text{A}$ .

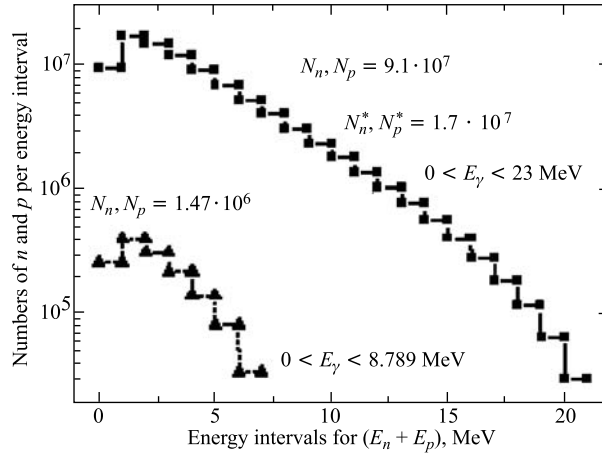


Fig. 3. Histograms with the number of neutrons and protons in seven energy ranges (at  $E_\gamma^{\max} = 9.3$  MeV) and 21 energy ranges (at  $E_\gamma^{\max} = 23$  MeV), respectively

The total yields of neutrons  $N_n$  and protons  $N_p$  and the numbers of  $N_p^*$  and  $N_n^*$  with energies  $E_n^* + E_p^* > (3.39 + 3.24)$  MeV (see below) are presented:  $N_n, N_p = 1.47 \cdot 10^6 \mu\text{A}^{-1}$  for  $E_\gamma < 8.789$  MeV and  $N_n, N_p = 9.1 \cdot 10^7 \mu\text{A}^{-1}$  and  $N_{n,p}^*(E_{n,p} > E_{n,p}^{\text{thresh}}) = 1.7 \cdot 10^7 \mu\text{A}^{-1}$  for reactions (18) and (19), which are presented below.

## 2. PHENOMENOLOGICAL NUCLEAR-REACTION DESCRIPTION

The following processes occur during the irradiation of targets with  $\gamma$  quanta, and the scenario of the so-called multiplication of the number of participating particles as «avalanche» of particles is as follows:

1. Dissociation processes of molecular deuterium into deuterium atoms and ions:



This process is very important because the absorption deuterium atom rate of most materials strongly depends on its atomization. Dissociation of D molecules to D atoms can be a very effective process only at the surface of the so-called Pd blackened surface [8]. In view of the heavy flux of quanta of small energies (see below), such processes can be effective.

2. Deuteron photodisintegration process (1) will be discussed below. The energy of photoprotons and photoneutrons must satisfy the energy conservation law:  $E_n + E_p = E_\gamma - \Delta W$ , where  $\Delta W = 2.22$  MeV is the deuteron binding energy. Thus, the momentum of  $\gamma$  quanta is small,  $p_\gamma = E_\gamma/c_0$ , where  $c_0$  is the velocity of light, then

$$E_n \approx E_p = 0.5(E_\gamma - \Delta W). \quad (8)$$

3. Moderation of neutrons from the photodisintegration energies down to thermal ones at the expense of deuteron elastic scattering, bound (in deuterides of palladium and other metals) and free (in deuterium gas). As is known, when fast neutrons of energy  $E_n > 0.1$  MeV are elastically scattered on deuterium, they become moderated. The efficiency criterion of neutron moderation is the average number of neutron collisions with the moderator nuclei at the moderation from the energy  $E_n^0$  down to  $E_n$  (see [8, p. 62]):

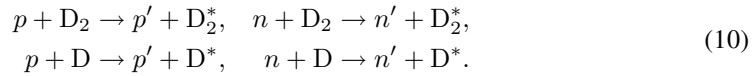
$$\bar{n} = \frac{\ln(E_n^0/E_n)}{\xi}, \quad (9)$$

where  $\xi$  is the mean logarithmic loss of neutron energy per one collision, which can be

represented as  $\xi = 1 + \frac{(A-1)}{2A} \ln \frac{A-1}{A+1}$ , where  $A$  is the moderator atomic mass unit (amu);

for deuterium,  $\xi = 0.725$ . Then the number of collisions at the moderation from 1 MeV down to 0.025 eV is  $\bar{n} = 24$ , while from 7 MeV down to 0.025 eV it amounts to  $\bar{n} = 27$  collisions. The average energy transferred to deuterons should be about  $\bar{E}_n \approx 3.4$  MeV/26  $\approx$  130 keV.

4. Elastic scattering of protons and neutrons from photodisintegration of deuterons with transfer energy to molecular and atomic deuterium:

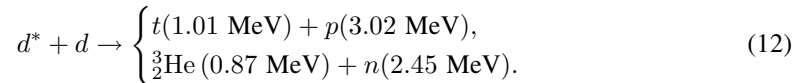


The maximal energy transferred by protons and neutrons to deuteron molecules and atoms in one collision is

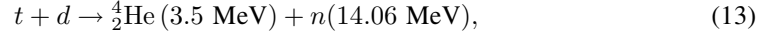
$$\begin{aligned} E_{D_2}^{\max} &= \frac{4M_{p,n}M_{D_2}}{(M_{p,n} + M_{D_2})^2} E_{p,n} = \frac{16}{25} E_{p,n}, \\ E_D^{\max} &= \frac{4M_p M_D}{(M_{p,n} + M_D)^2} E_{p,n} = \frac{8}{9} E_{p,n}. \end{aligned} \quad (11)$$

It is important to note that scattering of charge particles can also depend on structure and aggregate state of targets.

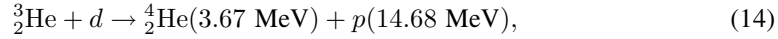
5. Processes of thermonuclear fusion of «hot» deuterons produced in reactions (10) and (11) with «cold» deuterons at rest in gas and in palladium (metal) saturated with deuterium:



6.  ${}^3_2\text{He}$  nuclei, tritons, protons and neutrons produced in reactions (12) can also take part in further reactions, both elastic and inelastic ones:



as well as in the reactions of deuterium heating  $d + D$ ,  $p + D$ ,  $n + D$  and



however, with a decreasing number of participating particles and decreasing cross sections in a series of reactions.

7. Processes of thermal neutron capture by atomic nuclei  ${}^A_Z N^Z(n, \gamma) {}^{A+1}_Z N$  with  $\gamma$ -quanta emission.

8. Photoemission of neutrons and protons from nuclei in giant resonance branch under  $\gamma$ -quanta absorption  ${}^A_Z N(\gamma, n) {}^{A-1}_Z N$  and  ${}^A_Z N(\gamma, p) {}^{A-1}_{Z-1} N$ .

9. Fission processes of atomic nuclei of middle masses induced by neutrons, protons and deuterons:  ${}^A_Z N(n, {}^{A_1}_{Z_1} N) {}^{A_2}_{Z_2} N$  (where  $A + 1 = A_1 + A_2$ ,  $Z = Z_1 + Z_2$ );  ${}^A_Z N(p, {}^{A_1}_{Z_1} N) {}^{A_2}_{Z_2} N$  (where  $A + 1 = A_1 + A_2$ ,  $Z + 1 = Z_1 + Z_2$ ) and  ${}^A_Z N(d, {}^{A_1}_{Z_1} N) {}^{A_2}_{Z_2} N$  (where  $A + 2 = A_1 + A_2$ ,  $Z + 1 = Z_1 + Z_2$ ) with the conservation of energy and momentum laws.

10. Elastic scattering of fission fragments on deuterium atoms with energy transfer to deuterium atoms using reactions (10) in dense deuterium gas and saturated metals atoms and with electronic excitations.

11. Of course, consideration should be given to a Coulomb barrier, which is equal to

$$E_Q \cong \frac{Z_1 Z_2 e_0^2}{\left(\sqrt[3]{A_1} + \sqrt[3]{A_2}\right) R_0} \text{ MeV}, \quad (15)$$

where  $R_0 = 1 \text{ fermi} = 10^{-13} \text{ cm}$ .

The calculated values of Coulomb barriers for Cu, Zn and Pd nuclei are presented in Table 2.

Table 2. Coulomb barriers for Cu, Zn and Pd nuclei

Reaction	$E_Q$ , MeV		
	102,104,105,106,108,110 46Pd	63,65 29Cu	64,66,67,68,70 30Zn
$p + {}^A_Z N$	$\sim 8.1$	$\sim 5.8$	$\sim 6.0$
$d + {}^A_Z N$	$\sim 7.5$	$\sim 5.5$	$\sim 5.7$

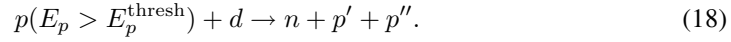
12. In order to estimate cross section and proton reaction yields, one can introduce the wavelength for a proton of energy  $E_p$  [4]:

$$\lambda = \frac{4.553 \cdot 10^{-3}}{E_p^{1/2}(\text{MeV})} \text{ cm}, \quad (16)$$

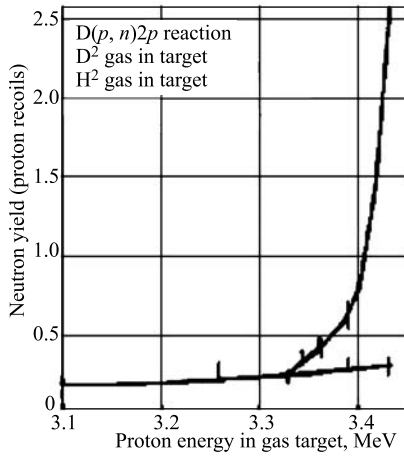
as well as the effective cross section  $\pi\lambda^2$  (b) [4]:

$$\sigma_{\text{eff}} = \pi\lambda^2 = \frac{0.6512}{E_p} \text{ b.} \quad (17)$$

13. Apart from this, in order to ensure interpretation of the obtained results, we have considered here additional deuteron disintegration reactions induced by protons with sufficient energy (reaction  $d(p, n)2p$ ) [9–11]:



The handbook [12] provides experimental results which are still being referred to and give such values for the energy threshold of reaction (18) as  $E_p^{\text{thresh}} = (3.340 \pm 0.015)$  MeV



and for the energy yield of the reaction as  $Q = (2.227 \pm 0.010)$  MeV. The cross section of reaction (18) at the proton energy near the threshold ( $E_p = 3.4$  MeV) is estimated as  $\sim 1 \mu\text{b}$  ( $10^{-30} \text{ cm}^2$ ) [9], but in an earlier study [10] for protons of energy  $E_p = 5.1$  MeV the cross section of reaction (18) was evaluated as  $\sim 0.014$  b ( $1.4 \cdot 10^{-26} \text{ cm}^2$ ). Figure 4 shows the cross section of reaction (18) near the reaction threshold. It is apparent that the energy of particles from reaction (18) must obey the expression  $E_n + E_{p'} + E_{p''} = E_p - E_p^{\text{thresh}}$ .

14. The reaction  $d(n, 2n)p$  with the cross section given in Fig. 5 can be realized likewise [13]:

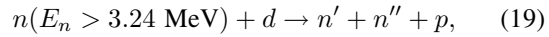


Fig. 4. Cross section of reaction (18) versus energy [11]

with the energies of all particles after decay described by the expression:  $E_{n'} + E_{n''} + E_p = E_n - E_n^{\text{thresh}}$ , where  $E_n^{\text{thresh}} = 3.29$  MeV.

With account of deuterium reactions induced by protons and neutrons from reactions (19) and (20) with relatively high energies, proton and neutron yields from electron beams with

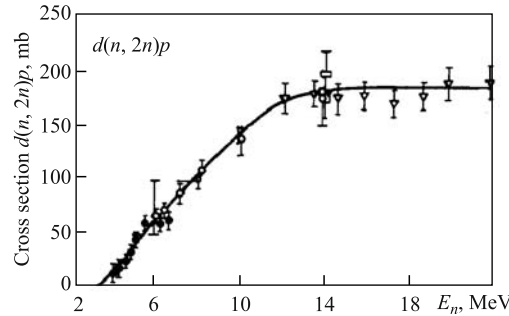


Fig. 5. Cross section of reaction (19) versus energy [13]

the current  $1 \mu\text{A}$  and energy  $E_\gamma = 25 \text{ MeV}$  are calculated to be  $N_{n,p}^*(E_{n,p} > E_{n,p}^{\text{thresh}}) = 1.7 \cdot 10^7 \mu\text{A}^{-1}$  (see Fig. 3). Fission reactions (18) and (19) take place with *multiplication of neutrons and protons, i.e., these are so-called chain reactions.*

15. Let us consider the subbarrier fusion reactions. We turn our attention now to the calculation of the cross section of nonresonance exothermic reactions between charged particles, which yields the following result:

$$\sigma(E) = \frac{C}{\sqrt{E}} \left\{ \sqrt{\frac{E_G}{E}} \exp\left(-\sqrt{\frac{E_G}{E}}\right) \right\} = \frac{S}{E} \exp\left(-\sqrt{\frac{E_G}{E}}\right), \quad (20)$$

where  $E_G = \frac{M}{2}(2\pi e_0^2 Z_1 Z_2 / \hbar)^2$  is the Gamow energy, while  $C$  and  $S$  are the parameters weakly dependent on the energy  $E$ . Clearly, the multiplier in braces from (20) describes the probability of a charged particle passing through the Coulomb energy barrier and is referred to as barrier permeability. The multiplier  $C/\sqrt{E}$  can be represented in the first approximation as a product of geometric cross section of collision, proportional to  $\pi R^2$ , by the probability of nuclear reaction where colliding particles are within the limit of the action of nuclear forces, i.e., at the distances  $r < R$ . This probability is proportional to the particle residence time in the region  $r < R$ , i.e., to the value  $R/v \sim 1/\sqrt{E}$  of decay probability of a compound nucleus by the required decay channel weakly dependent on  $E$ . The cross section of the  $d-d$  reaction at small energies can be presented in the form [15, 16]

$$\sigma_{d-d} = \frac{S(E)}{E} \exp\left(-\frac{31.4}{\sqrt{E}}\right), \quad (21)$$

with  $S(E)$  and  $E$  measured in  $\text{keV} \cdot \text{b}$  and  $\text{keV}$ , respectively.

The cross section calculated using the data presented in [15] is given in Table 3.

Table 3. Cross section of  $d-d$  reaction for small energy

Quantity	Energy, keV			
	4	8	14	21
$S$ -factor, $\text{keV} \cdot \text{b}$	140	72	64	56
Cross section, mb	$5.26 \cdot 10^{-3}$	$1.4 \cdot 10^{-1}$	1.0	2.8

Figure 6 shows energy dependences of cross sections of  $d-d$  and  $d-t$  fusion reactions [14].

As is seen, in spite of  $S$ -factor growth,  $d-d$  cross section decreases strongly with decreasing energy, but begins to grow quickly if the energy is more than about 10 keV (see also Table 3).

16. Let us consider the large differences between reactions of protons and neutrons with nuclei, which were explained by Oppenheimer and Phillips [18] using the orientation deuteron effect for the reaction:



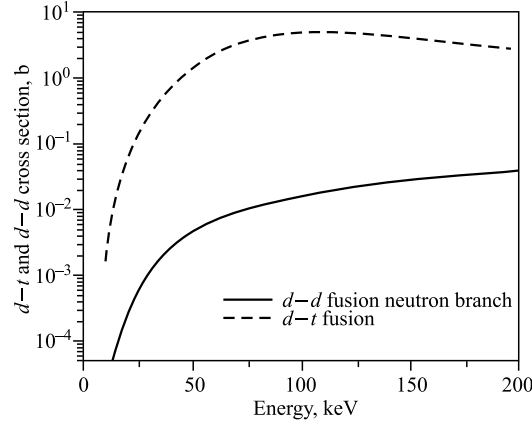


Fig. 6. Cross sections of deuterium–deuterium and deuterium–tritium reactions versus energy [14]

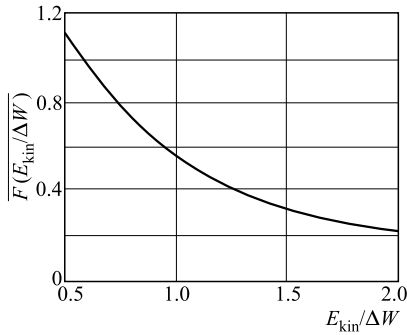


Fig. 7. Cross section versus energy  $E_{\text{kin}}/\Delta W$  for reaction (22) [18]

in a deuterium energy interval of about 0.5–2.0 MeV. The cross section of the reaction was obtained in the form

$$\sigma \approx \frac{1}{V^2} \exp \left[ -\frac{4Ze_0^2}{\hbar} \left( \frac{M}{\Delta W} \right)^{1/2} \overline{F \left( \frac{E_{\text{kin}}}{\Delta W} \right)} \right]; \quad (23)$$

the function  $\overline{F \left( \frac{E_{\text{kin}}}{\Delta W} \right)}$  is presented in Fig. 7 [18].

As well known [17], the thermal vibrations of lattice atoms should increase the effective cross section of elastic and inelastic scattering of charged particle into solid and gas targets mainly at low-energy scattering, because the vibrations should more effectively increase

the transverse cross section with increasing interaction time. This cross-section scattering dependence  $\sigma(E, T)$  should be more important when the temperature of solid target is close to melting temperature. Temperature dependences of energy transfer from heated electrons under passage of charged particles through solids to the lattice also depend on thermal vibrations.

It is also necessary to note the change of the scattering situation for crystalline and amorphous solids [17]. Chaotic arrangements of lattice atoms do not create periodic potential in the lattice, excluding low energy loss processes of particle scattering, such as channeling and so on. The difference for single crystal and amorphous targets is due to collision cross section  $\sigma$ . In the absence of periodic potential (amorphous target) gaseous cross section is equal to square Debye–Hückel length  $\sigma_{\text{amorph}} = \pi d^2 \approx 0.5 \cdot 10^{-16} \text{ cm}^2 = 5 \cdot 10^7 \text{ b}$ . In single crystal, this value is necessary to multiply by factor  $\alpha = \Theta/MS^2$ , where  $\Theta$ ,  $M$  and  $S$  are the temperature of lattice ( $\approx 2000^\circ\text{C}$ ), mass of lattice atoms and velocity of sound, respectively [17]. The velocity of sound is about  $3 \cdot 10^3 \text{ m/s}$ . The  $\alpha$  factor is about  $\alpha = 0.017$  for Pd atoms. Taking into consideration single-crystal structures of main solids, this factor should be  $0.017 < \alpha < 1.0$ . So the cross section for single crystal becomes  $\sigma_{\text{crys}} = \alpha \pi d^2 \approx 8.5 \cdot 10^5 \text{ b}$ .

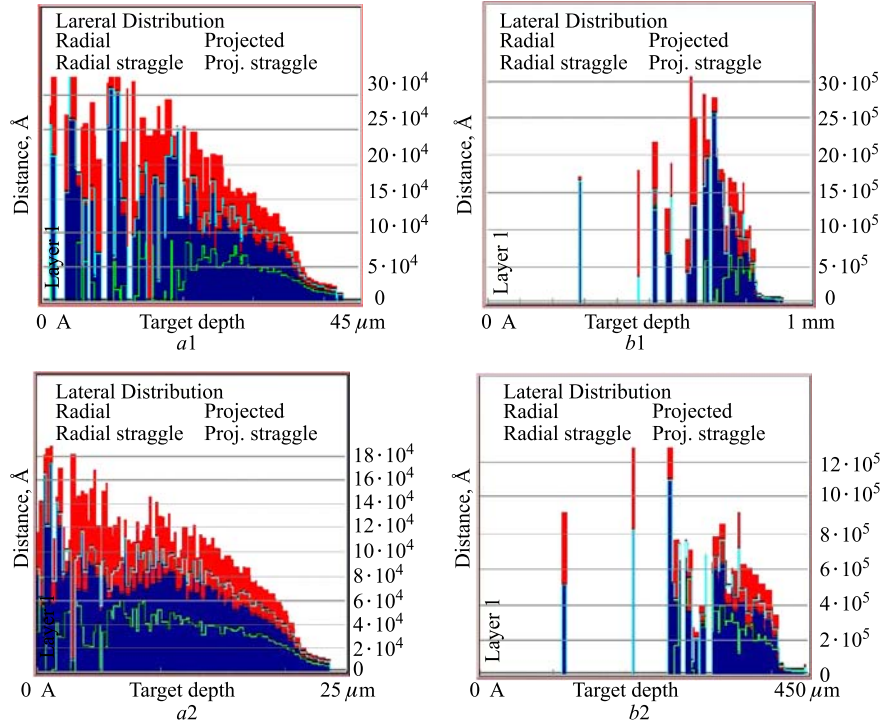


Fig. 8. Lateral distributions of  $p$  (energy is 3.3 MeV) and  $D$  (energy is 3.0 MeV) into 3 kbar dense deuterium gas ( $b1$ ,  $b2$ ) and  $Pd_{0.57}D_{0.43}$  ( $a1$  and  $a2$ ), respectively

The lateral projected ranges for protons (3.3 MeV) and for deuterium atoms (3.0 MeV) in 3 kbar deuterium dense gas and in  $Pd_{0.57}D_{0.43}$  solid target are presented in Fig. 8. It is seen that at deuterated palladium, protons and deuterons with these energies have relatively small projected ranges and also a lot of small projected ranges, and it means that the particle lost large part of its energy at collisions. It means that probabilities of direct heating of «cold» deuterium atoms by protons and hot deuterium atoms too are not small ones.

Let us calculate projected ranges of all particles which should be taken into consideration in dense deuterium gas (atomic  $n_D = 5.19 \cdot 10^{22}$  D/cm<sup>3</sup> and mass density  $\rho_D = 0.1713$  g/cm<sup>3</sup>) and palladium saturated by deuterium. The swelling of Pd rod was limited by DHPC walls from 3.8 to 4 mm, so we will take densities of Pd as  $n_D = 6.8 \cdot 10^{22}$  D/cm<sup>3</sup> and

Table 4. Projected ranges of  $p$  (3.4 MeV),  $d$  (3.02 MeV),  $^{50}_{22}Ti$  (5 MeV),  $t$  (1.02 MeV) and  $^3_2He$  (0.84 MeV) with numbers of D atoms along the particle paths using TRIM-2007 computer code

Target state	$p$ (3.3 MeV)	$d$ (3.0 MeV)	$^{50}_{22}Ti$ (5 MeV)	$t$ (1.02 MeV)	$^3_2He$ (0.84 MeV)
$D_2$ dense gas, $\mu m$	872	408	23.7	54.8	27.1
$R_p/r_{D-D}$	$3.25 \cdot 10^6$	$1.52 \cdot 10^6$	$8.84 \cdot 10^4$	$2.04 \cdot 10^5$	$1.01 \cdot 10^5$
$Pd_{0.57}D_{0.43}$ , $\mu m$	37.8	21.7	1.1	3.97	1.12
$R_p/r_{D-D}$	$1.41 \cdot 10^4$	$8.1 \cdot 10^4$	$4.10 \cdot 10^3$	$1.48 \cdot 10^4$	$4.18 \cdot 10^3$

$\rho_{\text{Pd}} \approx 12.02 \text{ g/cm}^3$ . Table 4 presents the calculated projected ranges of all particles with their maximum energies which should be created in reactions  $p(3.4 \text{ MeV})$ ,  $d(3.02 \text{ MeV})$ ,  ${}^{50}_{22}\text{Ti}$  (5 MeV),  $t(1.02 \text{ MeV})$  and  ${}^3_2\text{He}$  (0.84 MeV) and also the fission fragment (see points 5, 6)  ${}^{50}_{22}\text{Ti}$  (energy is about 5 MeV) with the numbers of D atoms along depth for each particle of interest only. The average distance between D–D atoms is equal to  $r_{\text{D-D}} = 1/\sqrt[3]{n_{\text{D}}} \cong 2.68 \text{ \AA}$ .

It is seen from Table 4 that the total lengths of deuterium atoms lines with a distance between D–D of about 2.68 Å are very long. And as well known, the diameter of H or D atoms is 1.058 Å. The relation between D–D distance (2.68 Å) and the diameter of atoms (1.058 Å) is very close.

So one can conclude all the above reactions which take place with different probabilities should be taken into consideration. The following *scenario of the process can be presented*: (a) deuterium disintegration reactions taking place under the action of 8.8 MeV  $\gamma$  quanta (1) (b) with production of relatively large energy protons and neutrons ( $E_n, E_p \subseteq 3.3 \text{ MeV}$ ), (c) which in their turn initiated subsequent heating of deuterium atoms (deuterons) with production of «hot» deuterons (10), d) which can cause a  $d-d$  disintegration reaction of deuterons (1) and following thermonuclear reactions (12)–(14), (e) the parallel reactions of «hot» deuterons with nuclei with transfer of neutrons to them, (f) which allow the process of fission of the compound nucleus to fission fragments and again with the formation of high-energy protons, (g) heating of deuterium atoms (deuterons) by energetic large-charge fission fragments and by again created «hot» protons.

### 3. NUCLEAR FISSION REACTIONS FOR DESCRIPTION OF MEASURED COMPOSITIONS OF DHPC

All reactions  ${}^A_Z N(\gamma, n){}^{A-1}_Z N$ ,  ${}^A_Z N(\gamma, p){}^{A-1}_{Z-1} N$ ,  ${}^A_Z N(n, \gamma){}^{A+1}_Z N$ ,  ${}^A_Z N(n, p){}^{A-1}_{Z-1} N$ ,  ${}^A_Z N(n, 2n){}^{A-1}_Z N$ ,  ${}^A_Z N(n, \alpha){}^{A-3}_{Z-2} N$  are very well measured, and their cross sections are very well known. Concerning fission nuclear reactions of middle-mass nuclei into light fission fragments, such reactions either have low probabilities as competition mode of nucleon decays or are impossible or unknown.

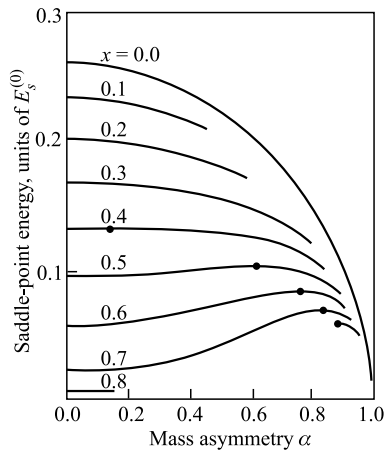


Fig. 9. Conditional-saddle-point energies (in units of the surface energy of a liquid-drop sphere) as a function of mass asymmetry  $\alpha$  and fissility  $x$ . The  $\alpha$  is the difference of the masses of the two nascent fragments divided by the total mass. The fissility  $x$  is one-half the ratio of the Coulomb energy of a sphere of uniform charge density to its surface energy

The results of chemical compositions of all measured components of DHPC [1, 2] allow one to conclude about strong chemical changes.

And we will discuss only *possible scenario of nuclear decays* inside the chamber under  $\gamma$  quanta and products of photodisintegration of deuterons. *The probable nuclear fission reactions, of course, are required taking into consideration the energy barriers of fission (see [22–24]).*

*Actually, the nature of the decay of highly excited compound nuclei is only qualitatively correct, since fission decays of any mass asymmetry are energetically allowed [23].* Let us present conditional-saddle-point energies (in units of the surface energy of a liquid-drop sphere) as a function of mass asymmetry in Fig. 9 [22].

**3.1. Reactions in Brass on Cu and Zn.** The  $(\gamma, n)$  reaction energies for all Cu and Zn isotopes were calculated and are presented in Table 5 using data of [7].

Let us also introduce the characteristics of  $(n, \gamma)$  reactions with Cu and Zn of thermal neutrons, which are presented in Table 6.

Table 5. Parameters of  ${}^A_{29}\text{Cu}(\gamma, n){}^{A-1}_{29}\text{Cu}^*$  and  ${}^A_{30}\text{Zn}(\gamma, n){}^{A-1}_{30}\text{Zn}^*$  reactions

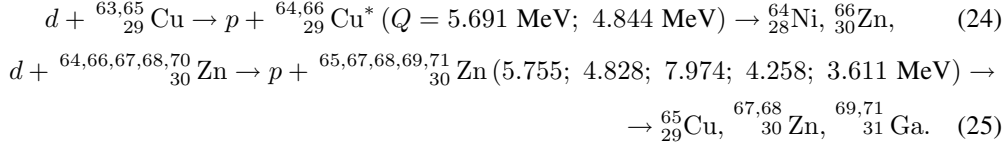
Element	Cross section, b	Abundance, % [7]	Final stable nucleon	Energy yield $Q$ , MeV
${}^{63}_{29}\text{Cu}$	Giant resonance	69.17	${}^{62}_{28}\text{Ni}$ (3.59%)	−10.854
${}^{65}_{29}\text{Cu}$	Giant resonance	30.83	${}^{64}_{28}\text{Ni}$ (0.91%)	−9.910
${}^{64}_{30}\text{Zn}$	Giant resonance	48.6	${}^{63}_{29}\text{Cu}$ (69.17%)	−11.862
${}^{66}_{30}\text{Zn}$	Giant resonance	27.9	${}^{65}_{29}\text{Cu}$ (30.83%)	−11.703
${}^{67}_{30}\text{Zn}$	Giant resonance	4.1	${}^{66}_{30}\text{Zn}$ (27.9%)	−7.053
${}^{68}_{30}\text{Zn}$	Giant resonance	18.8	${}^{67}_{30}\text{Zn}$ (4.1%)	−10.824
${}^{70}_{30}\text{Zn}$	Giant resonance	0.6	${}^{69}_{31}\text{Ga}$ (60.1%)	−9.857

Table 6. Parameters of  ${}^A_{29}\text{Cu}(n, \gamma){}^{A+1}_{29}\text{Cu}^*$  and  ${}^A_{30}\text{Zn}(n, \gamma){}^{A+1}_{30}\text{Zn}^*$  reactions

Element	Cross section $\sigma_{n, \gamma}$ , b [19, 20]	Abundance, % [7]	Final stable nucleon	Energy yield $Q$ , MeV
${}^{63}_{29}\text{Cu}$	4.50	69.17	${}^{64}_{28}\text{Ni}$ (0.91%)	+7.916
${}^{65}_{29}\text{Cu}$	2.17	30.83	${}^{66}_{30}\text{Zn}$ (27.6%)	+7.066
${}^{64}_{30}\text{Zn}$	0.76	48.6	${}^{65}_{29}\text{Cu}$ (30.83%)	+7.980
${}^{66}_{30}\text{Zn}$	0.85	27.9	${}^{67}_{30}\text{Zn}$ (4.1%)	+7.053
${}^{67}_{30}\text{Zn}$	6.8	4.1	${}^{68}_{30}\text{Zn}$ (18.8%)	+10.198
${}^{68}_{30}\text{Zn}$	0.072	18.8	${}^{69}_{31}\text{Ga}$ (60.1%)	+6.482
${}^{70}_{30}\text{Zn}$	0.083	0.62	${}^{71}_{31}\text{Ga}$ (39.9%)	+5.836

Let us try to find any reactions where light elements, which were measured at synthesized novel object (SNO), such as Al, Si and Ti, can be produced. All neutron ( $E_n < 3.4$  MeV) induced fission reactions with Cu and Zn are impossible ( $Q < 0$ ). Calculations of all subbarrier fusion reactions of energetic protons with Cu and Zn with production of  $\gamma$ , and light fission fragments are impossible too, because all reactions are endothermal ones.

Oppenheimer subbarrier reactions of  ${}_{29}\text{Cu}$  and  ${}_{30}\text{Zn}$  nuclei with deuterons (22) are possible, see, for example,



Accompanying chemical elements should be  ${}^{69,71}_{31}\text{Ga}$  and  ${}^{64}_{28}\text{Ni}$ . Proton energy should be  $E_p > \frac{M_{\text{Cu}}}{M_{\text{Cu}} + M_p} Q = 5.6 \text{ MeV}$  for the first reaction in (24). So, such subbarrier reactions can produce energetic protons and, in principle, fission fragments (for more detail, see [22–24]).

One can conclude that some of the reactions can produce chemical elements in SNO and no other chemical elements were observed! But any reactions with such an energy of  $\gamma$  quanta  $E_\gamma = 8.789 \text{ MeV}$  are not possible.

**3.2. Reactions in Pd Rod.** Tables 7 and 8 present characteristic parameters of  ${}^A_{46}\text{Pd}(\gamma, n){}^{A-1}_{46}\text{Pd}^*$  and  ${}^A_{46}\text{Pd}(n, \gamma){}^{A+1}_{46}\text{Pd}^*$  reactions.

Table 7. Parameters of  ${}^A_{46}\text{Pd}(\gamma, n){}^{A-1}_{46}\text{Pd}^*$  reactions

Element	Abundance, % [7]	Cross section, b [3, 19]	Final stable nucleon	Energy yield $Q$ , MeV
${}^{102}_{46}\text{Pd}$	1.020	Giant resonance	${}^{101}_{44}\text{Ru}$ (17.0%)	−10.568
${}^{104}_{46}\text{Pd}$	11.14	Giant resonance	${}^{103}_{45}\text{Rh}$ (100%)	−9.993
${}^{105}_{46}\text{Pd}$	22.33	Giant resonance	${}^{104}_{46}\text{Pd}$ (11.14%)	−7.093
${}^{106}_{46}\text{Pd}$	27.33	Giant resonance	${}^{105}_{46}\text{Pd}$ (22.33%)	−9.562
${}^{108}_{46}\text{Pd}$	26.46	Giant resonance	${}^{107}_{47}\text{Ag}$ (51.839%)	−9.190
${}^{110}_{46}\text{Pd}$	11.72	Giant resonance	${}^{109}_{47}\text{Ag}$ (48.161%)	−7.684

Table 8. Thermal neutron captures:  ${}^A_{46}\text{Pd}(n, \gamma){}^{A+1}_{46}\text{Pd}^*$  reactions

Element	Abundance, % [7]	Cross section, b [3, 19]	Final stable nucleon	$\gamma$ -quantum energy $Q$ , MeV
${}^{102}_{46}\text{Pd}$	1.020	3.4	${}^{103}_{45}\text{Rh}$ (100%)	7.624
${}^{104}_{46}\text{Pd}$	11.14	0.6	${}^{105}_{46}\text{Pd}$ (22.33%)	7.093
${}^{105}_{46}\text{Pd}$	22.33	20.0	${}^{106}_{46}\text{Pd}$ (27.33%)	9.562
${}^{106}_{46}\text{Pd}$	27.33	0.296	${}^{107}_{46}\text{Pd}$ ( $6.5 \cdot 10^6$ y)	6.529
${}^{108}_{46}\text{Pd}$	26.46	8.3	${}^{109}_{47}\text{Ag}$ (48.161%)	6.154
${}^{110}_{46}\text{Pd}$	11.72	0.190	${}^{111}_{48}\text{Cd}$ (12.80%)	5.765

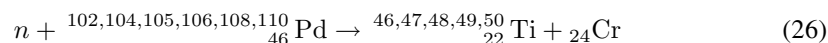
It is clear that only two photofission reactions should be with  ${}^{105}_{46}\text{Pd}$  and  ${}^{110}_{46}\text{Pd}$  because  $E_\gamma > |Q|$  (see also Table 7).

*It is important to note that the isotope composition of each chemical element observed after  $\gamma$ -quanta irradiation is the criterion of existence or absence of nuclear fission reactions.* So it is necessary for us to carry out accurate isotope mass separation analysis. And it should be the final proof of the developed approach.

Description of nuclear reactions for production of each chemical element lighter than  ${}_{46}\text{Pd}$ , which were determined during experimental studies of chemical compositions [1, 2] such as  ${}_{8}\text{O}$ ,  ${}_{9}\text{F}$ ,  ${}_{11}\text{Na}$ ,  ${}_{12}\text{Mg}$ ,  ${}_{13}\text{Al}$ ,  ${}_{14}\text{Si}$ ,  ${}_{15}\text{P}$ ,  ${}_{16}\text{S}$ ,  ${}_{17}\text{Cl}$ ,  ${}_{19}\text{K}$ ,  ${}_{20}\text{Ca}$ ,  ${}_{21}\text{Sc}$ ,  ${}_{22}\text{Ti}$ ,  ${}_{23}\text{V}$ ,  ${}_{24}\text{Cr}$ ,  ${}_{25}\text{Mn}$ ,  ${}_{26}\text{Fe}$ ,  ${}_{29}\text{Cu}$ ,  ${}_{30}\text{Zn}$ ,  ${}_{40}\text{Zr}$ ,  ${}_{41}\text{Nb}$ , and heavier ones  ${}_{44}\text{Ru}$ ,  ${}_{45}\text{Rh}$ ,  ${}_{47}\text{Ag}$ , and also volatile elements  ${}_{10}\text{Ne}$  and  ${}_{18}\text{Ar}$ , is very easy to write, because we have quite enough experimental data, but it is better to discuss only exact nuclear reactions which can be realized in DHPC under  $\gamma$ -quanta irradiations of deuterium-saturated palladium ( $\text{Pd}_{0.57}\text{D}_{0.43}$ ) and at the SNO.

The X-ray structural analysis allows us to conclude that SNO consists of three phases:  $\text{TiO}_2$  — titanium dioxide,  $\text{Pd}_{1.5}\text{D}_2$  — deuteride palladium and also something like titanium quartz phase.

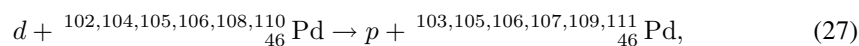
**Production of titanium:** it can be reactions with deuterons and neutrons:



with energies of reactions  $Q$  from 4.5 to 23.0 MeV and besides  ${}_{22}\text{Ti}$  in Pd rod should also be accompanied by elements  ${}_{24}\text{Cr}$ ,  ${}_{25}\text{Mn}$ ,  ${}_{26}\text{Fe}$ ,  ${}_{27}\text{Co}$ ,  ${}_{28}\text{Ni}$ ,  ${}_{29}\text{Cu}$ . It is very important to note that most of these atoms accompanying titanium were observed under SEM-microelement analysis [1, 2].

Fe and Cr were mainly observed at relatively large quantities in Pd rod irradiated with  $\gamma$  quanta [1, 2].

Also it can be reactions with deuterons (22), i.e.,



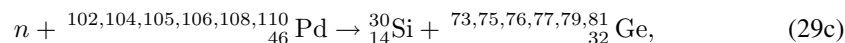
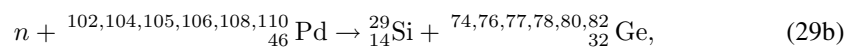
with energies of reactions  $Q = 5.3998; 4.8688; 7.3378; 4.3048; 3.9298; 3.5418$  MeV, respectively, and it would be probably nuclear fission under division with neutrons (see above).

**Aluminum production** under neutron and deuteron processes in which there can be produced chemical isotopes observed by SEM microelement analysis measurements:



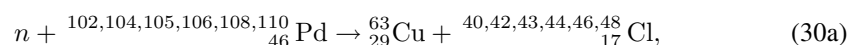
with energies of reactions  $Q$  from 3.09 to 10.564 MeV and with accompanying elements  ${}_{34}\text{Se}$  and volatile element  ${}_{36}\text{Kr}$ .

**Production of silicon atoms**  ${}^{28}_{14}\text{Si}$  (92.23%),  ${}^{29}_{14}\text{Si}$  (4.67%),  ${}^{30}_{14}\text{Si}$  (3.10%) under neutron division:



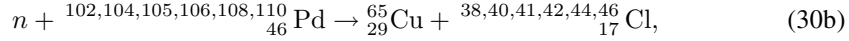
with the energies  $Q = 13.494; 11.377; 12.901; 9.220; 6.380; 7.018$  MeV for reactions, and  $Q = 15.462; 13.779; 12.757; 11.812; 9.971; 7.420$  MeV for reactions (29b), and  $Q = 15.872; 14.959; 17.295; 13.804; 12.550; 10.508$  MeV for reactions (29c) with accompanying elements  ${}^{73,74,76}_{32}\text{Ge}$ ,  ${}^{75}_{33}\text{As}$ ,  ${}^{77,78,79,80,82}_{34}\text{Se}$ ,  ${}^{81}_{35}\text{Br}$  and volatile element  ${}^{82,83,84}_{36}\text{Kr}$ .

**${}^{63}_{29}\text{Cu}$  production** under neutron division:



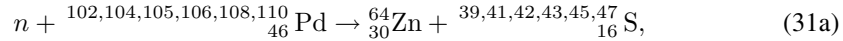
with energies of reactions  $Q = 13.265; 8.670; 8.368; 6.877; 7.267; 8.455$  MeV with accompanying element  $^{43,44,46,48}_{20}\text{Ca}$  and volatile element isotopes such as stable  $^{40}_{18}\text{Ar}$  and radioactive  $^{42}_{18}\text{Ar} \xrightarrow{\beta^-, \beta^-, 32,9 \text{ y}} ^{42}_{20}\text{Ca}$ .

**$^{65}_{29}\text{Cu}$  production** under neutron division:



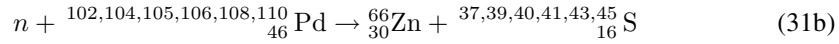
with energies of reactions  $Q = 17.206; 13.473; 14.311; 9.840; 8.950; 10.138$  MeV with accompanying elements  $^{41}_{19}\text{K}$ ,  $^{44,46}_{20}\text{Ca}$  and volatile elements  $^{38,40}_{18}\text{Ar}$  and  $^{42}_{18}\text{Ar}^*$  (see above).

**$^{64}_{30}\text{Zn}$  production** under neutron division:



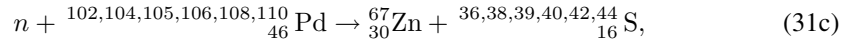
with energies of reactions  $Q = 9.148; 2.773; <3.751; <2.260; <2.650; <3.838$  MeV with accompanying elements  $^{41}_{19}\text{K}$ ,  $^{43}_{20}\text{Ca}$ ,  $^{45}_{21}\text{Sc}$ ,  $^{47}_{22}\text{Ti}$  and volatile elements  $^{39}_{18}\text{Ar}$  and  $^{42}_{18}\text{Ar}^*$  (see above).

**$^{66}_{30}\text{Zn}$  production** under neutron division:



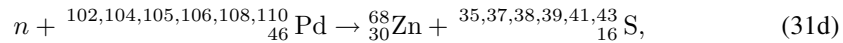
with energies of reactions  $Q = 15.953; 10.570; 10.788; 4.157; <5.547; <6.735$  MeV with accompanying elements  $^{37}_{17}\text{Cl}$ ,  $^{41}_{19}\text{K}$ ,  $^{43}_{20}\text{Ca}$ ,  $^{45}_{21}\text{Sc}$  and volatile element  $^{39,40}_{18}\text{Ar}$ .

**$^{67}_{30}\text{Zn}$  production** under neutron division:



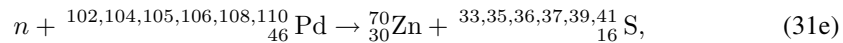
with energies of reactions  $Q = 18.692; 13.413; 10.529; 8.278; <4.528; <5.716$  MeV with accompanying elements  $^{36}_{17}\text{Cl}$ ,  $^{42,44}_{20}\text{Ca}$  and volatile elements  $^{38,39,40}_{18}\text{Ar}$  and  $^{42}_{18}\text{Ar}^*$  (see above).

**$^{68}_{30}\text{Zn}$  production** under neutron division:



with energies of reactions  $Q = 18.999; 15.586; 16.338; 11.165; 6.598; <7.843$  MeV with accompanying elements  $^{35,37}_{17}\text{Cl}$ ,  $^{41}_{19}\text{K}$ ,  $^{43}_{20}\text{Ca}$  and volatile element  $^{38,39}_{18}\text{Ar}$ .

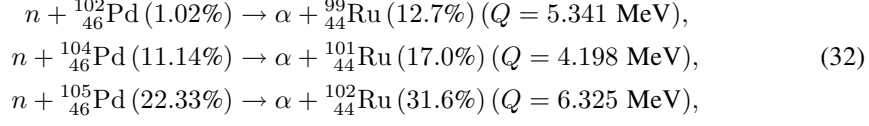
**$^{70}_{30}\text{Zn}$  production** under neutron division:



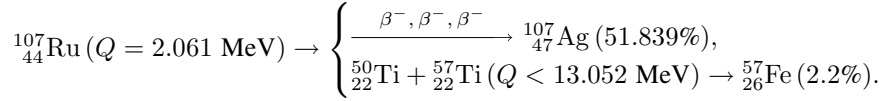
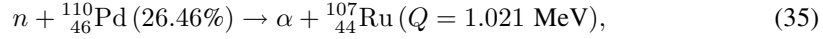
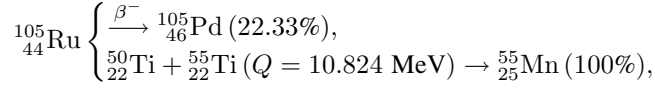
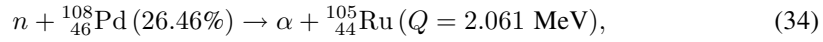
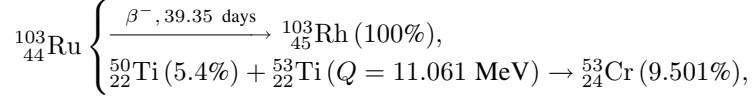
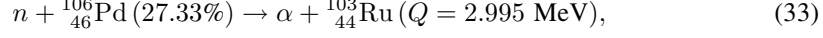
with energies of reactions  $Q = 16.292; 17.078; 19.875; 14.627; 11.108; 7.396$  MeV with accompanying elements  $^{33,36}_{16}\text{S}$ ,  $^{35,37}_{17}\text{Cl}$ ,  $^{41}_{19}\text{K}$  and volatile element  $^{39}_{18}\text{Ar}$ .

*So nuclear reactions of  $^{29}\text{Cu}$  and  $^{30}\text{Zn}$  production should be accompanied by isotopes  $^{33,36}_{16}\text{S}$ ,  $^{35,37}_{17}\text{Cl}$ ,  $^{41}_{19}\text{K}$ ,  $^{42,43,44,46,48}_{20}\text{Ca}$ ,  $^{45}_{21}\text{Sc}$  and  $^{47}_{22}\text{Ti}$ , but isotopes  $^{39,40}_{19}\text{K}$  and  $^{40}_{20}\text{Ca}$  should be absent! It is an excellent proof of the approach!*

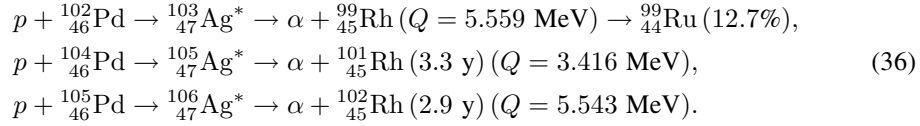
Let us consider reactions which can produce significant quantities of such elements as  ${}_{45}\text{Rh}$  and  ${}_{44}\text{Ru}$ . These nuclei can be produced by the reactions:



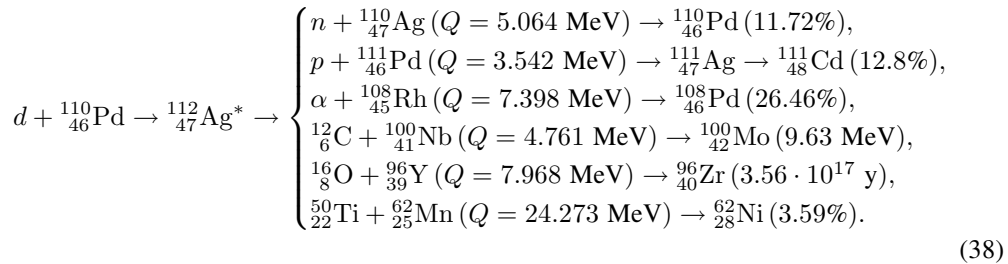
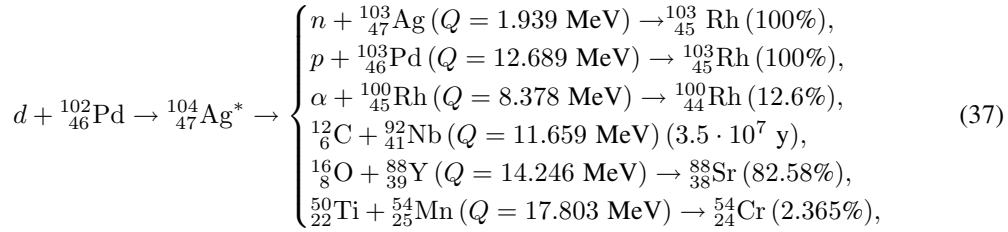
and some chain reactions:



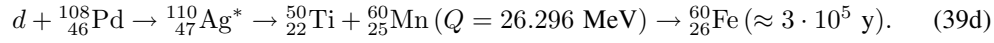
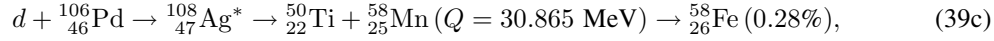
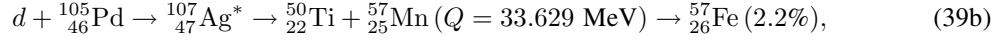
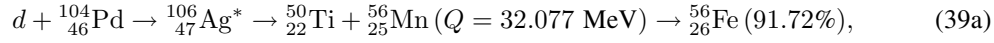
Let us consider some fission reactions with protons and deuterons, taking into consideration subbarrier fusion (see G. Gamov's expressions (2) and (21)):



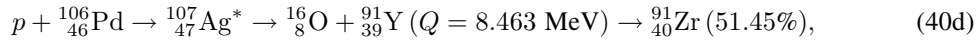
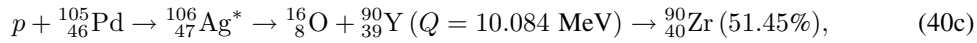
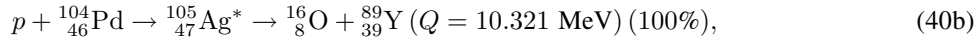
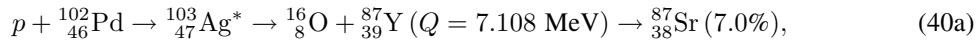
Let us consider some subbarrier exothermal reactions with deuterons:



Let us consider other reactions with production of titanium:



It is necessary to note that also inside DHPC a very large concentration of oxygen was observed and most part of SNO consists of rutile —  $\text{TiO}_2$  [1, 2]. As is well known, titanium is very oxidation-resistant metal, and its oxidation should be at large temperature and at dense oxygen atmosphere, but DHPC chamber was filled with 98% of deuterium and 2% of hydrogen mixture. Besides that, let us write some nuclear reactions with oxygen production during  $\gamma$ -quanta irradiation. These are some of such examples:

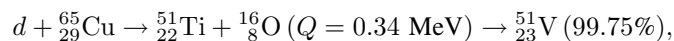
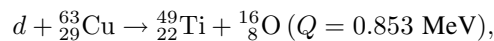
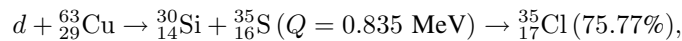
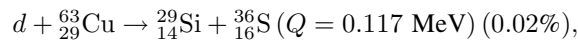


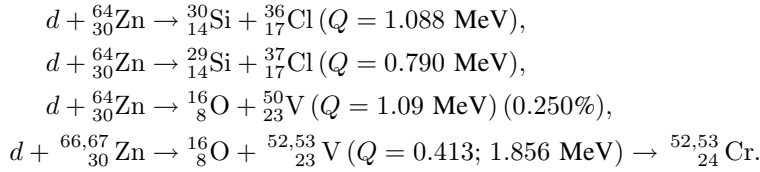
We now provide some reactions in which the measured chemical compositions can be produced. Also, for us it is very important to note that, using the developed scheme of nuclear chain reactions with multiplication of the number of «hot» deuterons and deuterium atoms and mainly «hot» protons together with «hot» fission fragments which can heat all components taking part in the process, it is possible to find reactions in which all measured composition can be described.

## CONCLUSIONS

We have shown the production of chain reactions of deuterium photofission–fusion reactions under  $\gamma$  quanta with power multiplication of protons and neutrons which stimulate fission of middle-mass nuclei into light fission fragments. It is important to note that the investigation of fusion and fission processes in highly dense deuterium under the action of various radiation sources, mainly  $\gamma$ -quanta irradiation, is a new area of fundamental research.

The reactions  $(\gamma, n)$ ,  $(n, f)$ ,  $(p, f)$  with copper and zinc at the energy of  $\gamma$  quanta  $E_\gamma < 8.8 \text{ MeV}$  are mainly absent. But reactions with multiplication of «hot» protons  ${}^A_Z N(d, p) {}^{A+1}_Z N$  and maybe  $(d, f)$  are suitable. Here « $f$ » refers to a fission reaction. Only subbarrier reactions with  $d$  are suitable for Cu and Zn:





The reactions with Pd isotopes with neutron production are as follows:  ${}^{105}_{46}\text{Pd}(\gamma, n) {}^{104}_{46}\text{Pd}$  ( $Q = -7.093 \text{ MeV}$ ),  ${}^{110}_{46}\text{Pd}(\gamma, n) {}^{109}_{46}\text{Pd}$  ( $Q = -7.684 \text{ MeV}$ )  $\rightarrow$   ${}^{109}_{47}\text{Ag}$  (48.161%) (see Table 7).

Let us consider reactions with  ${}_{22}\text{Ti}$  production. All the reactions with neutrons have the reaction yield  $Q > 15 \text{ MeV}$  and the final fission fragments should be  ${}_{24}\text{Cr}$ ,  ${}_{25}\text{Mn}$ ,  ${}_{26}\text{Fe}$ ,  ${}_{27}\text{Co}$ ,  ${}_{28}\text{Ni}$  [1, 2]. The reactions of  ${}_{29}\text{Cu}$  and  ${}_{30}\text{Zn}$  production  ${}^A_{46}\text{Pd}(n, {}^A_{29}\text{Cu}) {}^A_{17}\text{Cl}$  and  ${}^A_{46}\text{Pd}(n, {}^A_{30}\text{Zn}) {}^A_{18}\text{Ar}$  at conservation law  $A + 1 = A_1 + A_2$  can produce the following isotopes:  ${}^{33,36}_{16}\text{S}$ ,  ${}^{35,37}_{17}\text{Cl}$ ,  ${}^{38,39,40,42}_{18}\text{Ar}$ ,  ${}^{41}_{19}\text{K}$ ,  ${}^{42,43,44,46,48}_{20}\text{Ca}$ .

It is important to note that more abundant isotopes such as  ${}^{39}_{19}\text{K}$  (93.2581%) and  ${}^{40}_{20}\text{Ca}$  (96.941%) are to be absent under the isotope composition analysis. Also, the reactions of subbarrier fission with  $p, d$  and Pd isotopes can produce the observed isotopes  ${}_{45}\text{Ru}$ ,  ${}_{45}\text{Rh}$ ,  ${}_{41}\text{Nb}$ ,  ${}_{40}\text{Zr}$ ,  ${}_{26}\text{Fe}$ ,  ${}_{24}\text{Cr}$ ,  ${}_{22}\text{Ti}$  and in large quantities  ${}_{8}\text{O}$  [1, 2].

Thus, it is possible to present the following scenario of process development:  $\gamma$  quanta play the role of initiator of chain fusion–fission processes: 1) produce deuterium atoms with increasing of pressure inside the DHPC; 2) divide deuterons to high-energy protons and neutrons; 3) these photoprotons and photon neutrons can repeatedly transfer their energies in elastic scattering processes to deuterium atoms; 4) «hot» deuterium atoms can interact with «cold» deuterium in fusion processes with production of fusion fragments ( $p, n, t$  and  ${}^3_2\text{He}$ ); 5) another branch of «hot» deuteron interactions is the interaction with Pd nuclei using Oppenheimer's process with creation of large charge fission fragments and again «hot» protons; 6) such products, in their turn, can heat deuterium atoms and interact with each other with fusion processes between deuterium atoms. All these steps result in strong multiplication of «hot» deuterium and hydrogen atoms and «hot» deuterium atoms which can simultaneously divide middle-mass nuclei into fission fragments.

We estimate the energy efficiency of the observed phenomena as

$$\eta_{\text{HPC}} \cong \frac{E_{\text{SNS}} + E_{\text{Pd}} + E_{\text{fusion}} + Q}{\beta \Delta E_{\text{MT-25}}}, \quad (41)$$

where  $E_{\text{SNS}}$ ,  $E_{\text{Pd}}$ ,  $E_{\text{fusion}}$  and  $Q$  are the nuclear fission energies for Ti, Cu and Zn production in the Pd-rod surface, for fusion reactions and for heating of all elements inside the DHPC up to very high temperatures, respectively. The SNS volume in it is  $V_{\text{SNS}} \sim (1.5-1.9) \cdot 10^{-3} \text{ cm}^3$ . Let us take the SNS atomic density as  $n_{\text{SNS}} \approx (5-8) \cdot 10^{22} \text{ at./cm}^3$ . The total number of atoms in the SNS should then be  $N_{\text{SNS}} \approx (7.5-15.2) \cdot 10^{19}$  atoms. The minimal concentration of Ti atoms in the SNS can be estimated as  $C_{\text{Ti}} \approx 0.0526$  (see Ti atom concentrations at various points of the SNS structure: at the top — 5.26 at.%, in the melt around the volcanic crater — 2.47 at.% and on the crater floor about 50.65 at.%). As was evaluated above, in nuclear reactions producing titanium the energy yield per one fission act of compound nucleus makes up  $\Delta E_{\text{Ti}} \sim 10 \text{ MeV}$ ; therefore, the energy gained from generation

of titanium nuclei in the SNS structure is  $E_{\text{SNS}} \approx C_{\text{Ti}} N_{\text{SNS}} \Delta E_{\text{Ti}} = (0.626-1.270) \cdot 10^7$  J. The energy for production of Cu atoms with the concentration  $C_{\text{Cu}} \approx 0.3$  in the modified Pd-rod blackened layer with the volume  $V_{\text{Pd}} \approx 1.03 \cdot 10^{-3}$  cm<sup>3</sup> (the layer thickness is 82  $\mu\text{m}$ , the diameter is 0.38 cm) is equal to  $E_{\text{Pd}} \approx C_{\text{Cu}} N_{\text{Pd}} \Delta E_{\text{Cu}} \approx (0.36-0.576) \cdot 10^7$  J. The energy production from fusion reactions (12)–(14) can be estimated as  $E_{\text{fusion}} \approx [N_{\text{Cu}} + N_{\text{Ti}}] \cdot 0.5(3.32 + 4.03)$  MeV =  $(0.33-0.615) \cdot 10^7$  J. Thus, the total energy extraction  $E_{\text{tot}} = E_{\text{SNS}} + E_{\text{Pd}} + E_{\text{fusion}} \approx (1.2-2.3) \cdot 10^7$  J. The electrical power of the MT-25 accelerator is approximately 20 kW, which corresponds to the energy spent during the experiment in the time  $T \approx 2.22 \cdot 10^4$  s:

$$\Delta E_{\text{MT-25}} \approx 20 \text{ kW} \cdot 2.2 \cdot 10^4 \text{ s} = 4.4 \cdot 10^8 \text{ J.}$$

So, the efficiency should be much higher:  $\eta_{\text{HPC}} > 1$ .

The elaborated approach can be used as a fundamental basis for the novel type of deuterated nuclear fission reactors (DNFR) with high efficiency [8]. A deuterated Pd metal simultaneously plays the role of a moderator and absorber of neutrons. Such a DNFR can be compact and inexpensive, and may be replaced with fission reactors based on enriched uranium. Non-enriched uranium itself can serve as a «fuel» in a DNFR since uranium absorbs up to three deuterium atoms per one uranium atom (UD<sub>3</sub> [1, 2, 8]). The studies into the fission of nuclei with middle-mass number, initiated and being actively developed by the authors, will be continued towards increasing deuterium gas pressure, however, up to such values at which saturation of used substance can be reached up to its stoichiometric deuterium composition. For example, UD<sub>3</sub>, NbD<sub>2</sub>, TaD, VD<sub>2</sub> and rare-earth metals (Rem) form trideuteride compounds RemD<sub>3</sub>.

*The final scenario of the process can be presented:* (a) deuterium disintegration reactions taking place under the action of 8.8-MeV  $\gamma$  quanta (1) (b) with production of relatively large energy protons and neutrons ( $E_n, E_p \subseteq 3.3$  MeV), (c) which in their turn initiate following heating of deuterium atoms (deuterons) with production of «hot» deuterons (10), (d) which can cause a  $d-d$  disintegration reaction of deuterons (1) and following thermonuclear reactions (12)–(14), (e) the parallel reactions of «hot» deuterons with nuclei with transfer of neutrons to them and again production of more heated protons, (f) which allow the process of fission of the compound nucleus to fission fragments, and again with the formation of high-energy protons, (g) heating of deuterium atoms (deuterons) by energetic large-charge fission fragments and by newly created «hot» protons.

#### REFERENCES

1. *Didyk A. Yu., Wisniewski R.* Chemical Composition and Structural Phase Changes of Pd Sample and Properties of Novel Synthesized Structure at Dense Deuterium Gas under Irradiation by  $\gamma$  Quanta. JINR Preprint E15-2012-34. Dubna, 2012. 30 p.
2. *Didyk A. Yu., Wisniewski R.* Nuclear Reactions in Gaseous Deuterium under High Pressure and in Palladium Saturated with Deuterium Induced by  $\gamma$  Quanta // Lett. J. Explor. Front. Phys. — EPL. 2012. V. 99. P. 22001.
3. *Ishkhanov B. A., Kapitonov I. M.* Electromagnetic Interaction with Atomic Nuclei. M.: Moscow State Univ., 1979. P. 215.

4. *Bethe H., Morisson Ph.* Elementary Nuclear Theory. N.Y.: John Wiley & Sons, Inc.; London: Chapman & Hall, Limited, 1956. 356 p.
5. *Zhuchko V.E., Zen Chan Uk.* Polynomial Representation of Thick-Target Bremsstrahlung Spectra for Electrons of Energy 10–22 MeV // *At. Energy*. 1985. V. 59, No. 1. P. 65–66 (in Russian).
6. *Tarasko M.Z., Soldatov A.S., Rudnikov V.E.* Description of Thick-Target Bremsstrahlung Spectra for Electrons of Energy 4–12 MeV // *At. Energy*. 1986. V. 65, No. 4. P. 290–291 (in Russian).
7. *Physical Values: Handbook / Eds.: I. S. Grigoriev and E. Z. Mejlikhov.* M.: Energoatomizdat, 1991. 1232 p.
8. *Metal Hydrides / Editors and major contributors: W. M. Mueller, J. P. Blackledge, G. G. Libowitz.* N. Y.; London: Acad. Press, 1968. 429 p.
9. *Smyth R. V., Martin H. D.* Deuteron ( $p, n$ ) Threshold and the Deuteron Binding Energy // *Phys. Rev.* 1950. V. 77. P. 752.
10. *Smyth R. V., Richards H. T.* Deuterium ( $pn$ ) Threshold // *Phys. Rev.* 1948. V. 74. P. 1871.
11. *Barkas W. H., White M. G.* Disintegration of Deuterium by Protons and  $p-n$  Reactions in Gaseous Elements // *Phys. Rev.* 1939. V. 56. P. 288.
12. *Experimental Nuclear Physics. V. 1 / Ed. E. Segre.* N. Y.; London, 1953. 662 p.
13. *Cross-Section of Threshold Reactions, Induced by Neutrons: Handbook.* Energoatomizdat, 1982. 216 p.
14. *Gillich D. J., Kovanen A., Danon Y.* Deuterated Target Comparison for Pyroelectric Crystal D–D Nuclear Fusion Experiments // *J. Nucl. Mater.* 2010. V. 405. P. 181–185.
15. *Raiola F. et al.* Enhanced  $d(d, p)t$  Fusion Reactions in Metals // *J. Phys. G*. 2005. V. 31. P. 1141; *Eur. Phys. J. A*. 2006. V. 27, No. 01. P. 79.
16. *Bystritsky V. M. et al.* Measurements of Astrophysical  $S$  Factor and Screening Potential for  $d(d, n)^3\text{He}$  Reaction in  $\text{ZrD}_2$ ,  $\text{TiD}_2$ ,  $\text{D}_2\text{O}$  and  $\text{CD}_2$  Targets in the Ultralow Energy Region Using Plasma Accelerators // *Nucl. Phys.* 2012. V. 75, No. 1. P. 56.
17. *Yavlinskii Yu.* Track Formation in Amorphous Metals under Swift Heavy Ion Bombardment // *Nucl. Instr. Meth. B*. 1989. V. 146. P. 142–146.
18. *Oppenheimer J. R., Phillips M.* Note for the Transmission Functions for Deuteron // *Phys. Rev.* 1935. V. 48, No. 15. P. 500–502.
19. *Ishkhanov B. A. et al.* Cross-Sections of Photon Absorption by Atomic Nuclei with the Numbers of Nucleons 12–65. SINP MSU Preprint 2002-27/711. M., 2002. 22 p.
20. *Holden N. E.* Neutron Scattering and Absorption Properties. Brookhaven National Laboratory. Upton, New York 11973. 1996.
21. *Nuclear Wallets Cards.* Brookhaven National Laboratory / Ed. J. K. Tuli. 2005. 78 p.
22. *Sierk A. J.* Mass-Asymmetric Fission of Light Nuclei // *Phys. Rev. Lett.* 1985. V. 55, No. 6. P. 582–583.
23. *Sierk A. J.* Macroscopic Model of Rotating Nuclei // *Phys. Rev. C*. 1986. V. 33, No. 6. P. 2039–2053.
24. *Moretto L. G.* Statistical Emission of Large Fragments: A General Theoretical Approach // *Nucl. Phys. A*. 1975. V. 247. P. 211–230.

Received on April 4, 2012.